Supplemental material to:

Title: Impaired bile secretion promotes hepatobiliary injury in Sickle Cell Disease.

Authors: Ravi Vats[1], Silvia Liu[2,7], Junjie Zhu[3], Dhanunjay Mukhi[4], Egemen Tutuncuoglu[1], Nayra Cardenes[1], Sucha Singh[2], Tomasz Brzoska[1], Karis Kosar[2], Mikhil Bamne[5], Jude Jonassaint[5], Adeola Adebayo Michael[2], Simon C. Watkins[4], Cheryl Hillery[5,6], Xiaochao Ma[3,7], Kari Nejak-Bowen[2,7], Mauricio Rojas[1,4], Mark Gladwin[1,4,5,7], Gregory Kato[1,4,5], Sadeesh Ramakrishnan[4,7], Prithu Sundd[1,4,5,7], Satdarshan Pal Monga[2,4,7*], Tirthadipa Pradhan-Sundd[1,4,5,7*]

Affiliations:

1. Pittsburgh Heart, Lung and Blood Vascular Medicine Institute, University of Pittsburgh School of Medicine, Pittsburgh, PA.
2. Dept. of Pathology, University of Pittsburgh School of Medicine, Pittsburgh, PA.
3. Center for Pharmacogenetics, Department of Pharmaceutical Sciences, School of Pharmacy, University of Pittsburgh, Pittsburgh, PA
4. Department of Medicine, University of Pittsburgh School of Medicine, Pittsburgh, PA
5. Sickle Cell Center for Excellence, University of Pittsburgh School of Medicine and University of Pittsburgh Medical Center, Pittsburgh, PA.
6. Department of Pediatrics, UPMC Children's Hospital of Pittsburgh, Pittsburgh, PA.
7. Pittsburgh Liver Research Center, University of Pittsburgh School of Medicine and University of Pittsburgh Medical Center, Pittsburgh, PA.

*To whom correspondence should be addressed:

Tirthadipa Pradhan-Sundd, PhD

Research Assistant Professor

Dept. of Medicine, Division of Hematology-Oncology

University of Pittsburgh School of Medicine

E1225 BST, 200 Lothrop Street, Pittsburgh, PA, 15261

Email: tip9@pitt.edu

Satdarshan P. S. Monga, MD, FAASLD.

Endowed Chair for Experimental Pathology

Director: Pittsburgh Liver Research Center,

Professor of Pathology (EP) & Medicine (Gastroenterology, Hepatology & Nutrition)

Assistant Dean and Co-Director: Medical Scientist Training Program

University of Pittsburgh, School of Medicine

200 Lothrop Street S-422 BST,

Pittsburgh, PA 15261

Tel: (412) 648-9966; Fax: (412) 648-1916; E-mail: smonga@pitt.edu

Table of contents

Supplemental Methods

Animals

Townes SCD mice (SS, homozygous for $Hba^{tm1(HBA)Tow}$, homozygous for $Hbb^{tm2(HBG1,HBB*)Tow}$) and non-sickle control mice (AS, homozygous for $Hba^{tm1(HBA)Tow}$, compound heterozygous for $Hbb^{tm2(HBG1,HBB*)Tow}$/$Hbb^{tm3(HBG1,HBB)Tow}$) were obtained from the Jackson Laboratory (Bar Harbor, ME) and housed in a specific pathogen-free animal facility at the University of Pittsburgh. All animal experiments were approved by the Institutional Animal Care and Use Committee at the University of Pittsburgh Genotyping was performed by polymerase chain reaction (PCR) analysis using genomic DNA isolated from a tail clipping. Livers from age- and sex-matched mice were used as indicated in results. All mice used in the study were also 12-15 weeks old. Three or more mice were assessed at all given time points. All animal experiments and procedures were performed according to the guidelines of the NIH.

Histology, immunohistochemistry (IHC) and immunofluorescence (IF)

Tissue sections (4-6μm) were stained with hematoxylin and eosin (H&E). IHC on paraffin-embedded sections was performed on livers as described elsewhere. Primary antibodies used were against Ki-67, CK-19 (Thermo Scientific, Freemont, CA,) P21, NFkB (P65) (Cell Signalling) Sox-9, EpCAM, (Invitrogen) F4/80, TUNEL, CD45 and αSMA, (ABCAM). Secondary antibodies were horse anti-mouse (Vector Laboratories, Inc., Burlingame, CA), goat anti-rabbit, and donkey anti-goat (Chemicon, Temecula, CA), all used at a 1:400 dilution. Sections were stained for Nikon A1 Spectral Confocal microscopes were used to capture images. Nikon NLS software was used to analyze the data.

Western Blot

Immunoblotting was performed as described elsewhere[26]. The following primary antibodies were used: NFkB (p65) (1:1000, Santa Cruz), FXR (1:1000, Santa Cruz), RXR (1:300, Santa Cruz), FAS, TRAF-1(1:1000, Santa Cruz). Membranes were 4 washed five times for 5m each in TBST before being probed with HRP–conjugated secondary antibodies (1:5000 diluted in TBST; Santa Cruz Biotechnology) for 1.5h at room temperature. Membranes were washed three times for 10m each in TBST and visualized using the Enhanced Chemiluminescence System (GE Healthcare).

Immunoprecipitation (IP).

Lysate (500μg) in a 1-mL volume (in the presence of protease and phosphatase inhibitors) was incubated with primary antibody for 2h at 4°C using end-over-end rotation, followed by 50μL of resuspended protein A/G agarose for 1.5h. The pellets were collected by centrifugation (1000×g) and washed four times for 5m each with RIPA buffer at 4°C. The pellets were resuspended in an equal volume of standard electrophoresis loading buffer with SDS and fresh β-mercaptoethanol and boiled for 10 minutes. Samples (30μL) were resolved on premade ready gels. Antibodies used for IP were NFkB (p65) (1:1000, Santa Cruz), FXR (1:1000, Santa Cruz), RXR (1:300, Santa Cruz).

mRNA isolation and real time polymerase chain reaction

mRNA was isolated and purified from livers of AS and SCD mice (n=3/group). mRNA was isolated using Trizol (Invitrogen). RT-PCR was performed as described elsewhere[28]. Changes in target mRNA were normalized to GAPDH mRNA for each sample and presented as fold-change

over the average the respective control group. Each sample was run in triplicate. Sequences of primers used in this study are available on request.

Total Bile acid analysis

Hepatic total bile acids were measured using a total bile acids kit from Crystal Chem (Downers Grove, IL), as per the manufacturer's instructions. Briefly, frozen liver tissue was homogenized in 70% ethanol at room temperature and then incubated in tightly capped glass tubes at 50°C for 2 hrs. The homogenates were then centrifuged at 6,000*g* for 10 minutes to remove debris. Total bile acid levels were measured and concentrations determined using the calibration curve and mean change in absorbance value for each sample.

NAC treatment

Mice were administered NAC (2gm/kg) via drinking water for upto 12 weeks.

Hydroxyproline Assay

To measure the hydroxyproline content in liver samples 500 µL of 6 N HCl was added to 50 mg of liver tissue and incubated at 100°C for 24 hours, followed by neutralization with 500 µL 6 N NaOH. The samples were then centrifuged at 13,000*g* for 12 minutes followed by incubating 120 µL of sample with 75 µL of chloramines T solution for 10 minutes. Finally 450 µL of perchloric acid/ para-dimethylaminobenzaldehyde/isopropranolwere added to each samples and were incubated for 30 minutes at 65°C and read at an absorbance of 561 nm.

Surgical preparation and qLIM imaging

Details of the surgical method are described here[15]. Intravascular fluorescent dyes included 200 μg of TXR dextran, or 100 μg of Carboxyflurescein (CF). TXR dextran/ (MW 70,000) was used to visualize the blood flow through the liver sinusoids whereas CF (Molecular weight 377) [15] was used to visualize uptake of the dye from blood to hepatocytes 3m post-injection and then from the hepatocyte to the bile-canaliculi within 5-8m. Microscopy was performed using a Nikon MPE multi-photon excitation microscope. The percentage of regions with vaso-occlusion (as seen by TXR-Dextran staining) per field of view (FOVs) was quantified. 10 FOVs were used on average/mice and the total number of liver sinusoidal vaso-occlusions per FOV, the percent of FOVs with vaso-occlusions, the area of vaso-occlusions were quantified.

Image Analysis

Movies were processed using Nikon's NIS Elements (Nikon Elements 3.10). A median filter with a kernel size of 3 was applied over each video frame to improve signal-to-noise ratio. Signal contrast in each channel of a multicolor image was further enhanced by adjusting the maxima and minima of the intensity histogram of that channel.

RNA seq analysis:

Liver were pelleted and lysed with RLT Buffer (Qiagen). RNA was isolated from the lysate using RNEasy kits (Qiagen). Library preparation, sequencing, and bioinformatics analysis were

performed by the Medgenome (CA, USA). Total RNA was processed for next-generation sequencing and sequencing was performed with a HiSeq 2500 (San Diego, CA, USA). Clontech SMARTer® UltraTM Low Input RNA Kits (Mountain View, CA, USA) and NexteraXT (San Diego, CA, USA) kits were used for library preparation.

Measurement of primary and secondary bile acid composition:

Liver samples were homogenized in water (100 mg tissue in 400 mL water), and then a 200 mL aliquot of methanol was added to 100 mL of liver homogenate. The mixture was vortexed twice for 1 min and centrifuged at 15,000xg for 20 minutes. It was then dissolved in acetonitrile: H2O (1:1; 2 μL in 1000 μL), vortexed for 30 seconds, and centrifuged at 15,000xg. One microliter of the supernatants from all samples was injected onto the ultra-performance liquid chromatography and quadrupole time-of-flight mass spectrometry (UPLC–QTOFMS) for analysis.

Statistical Analysis

All comparisons between two groups were deemed statistically significant by unpaired two-tailed Student's t-test if $p<0.05$(*) or $p<0.001$ (**). When more than two groups were compared, statistical analysis was performed with Prism version 7.0a (GraphPad Software) using one-way and two-way ANOVA with Bonferroni correction. All in vitro studies are either compilation of three-independent experiments or presented data is representative of at least three independent experiments.

Supplemental Figure and legends:

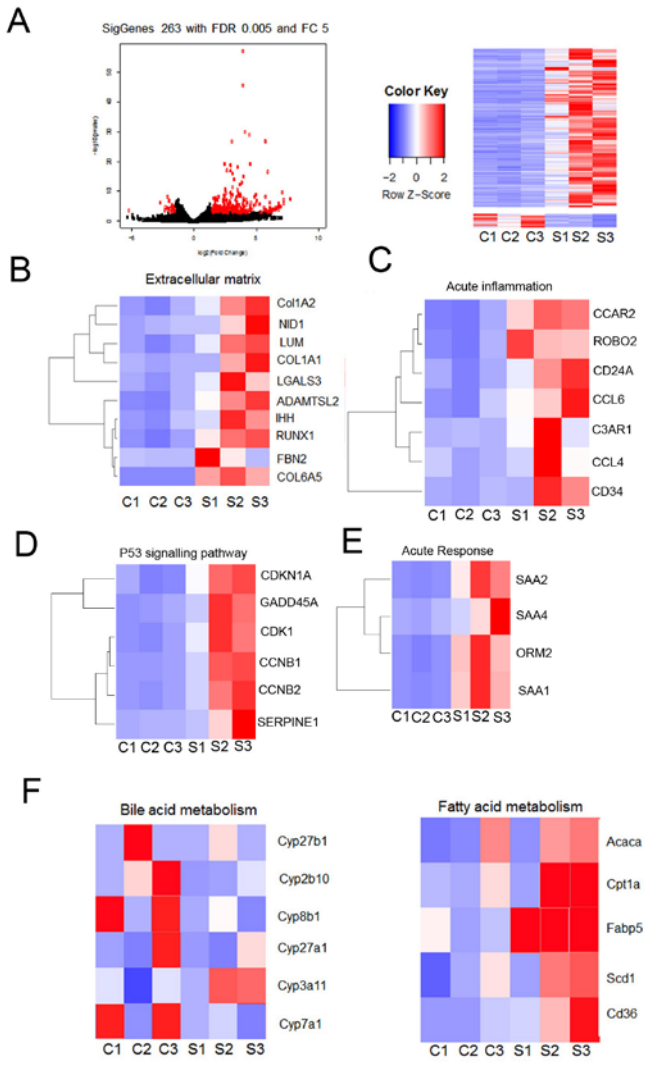

Figure S1: RNA sequence analysis of SCD liver exhibits misexpression of genes involved in inflammation and bile secretion. (**A**) Scatter plot of the RNA-seq data analysis between control and SCD mice liver. Heatmap of hierarchical clustering indicate differentially expressed genes (rows) between control and SCD mice (n=3), FDR=0.05 and fold change =5. (**B-E**) Pathway analysis revealed increased expression of genes involved in (**B**) extracellular matrix and fibrosis, (**C**) Acute inflammation, (**D**) P53 signalling pathway and (**E**) Acute response in the liver of SCD mice. (**F**) Heat maps showing differential expression of genes involved in bile acid and fatty acid metabolism in control and SCD mice liver.

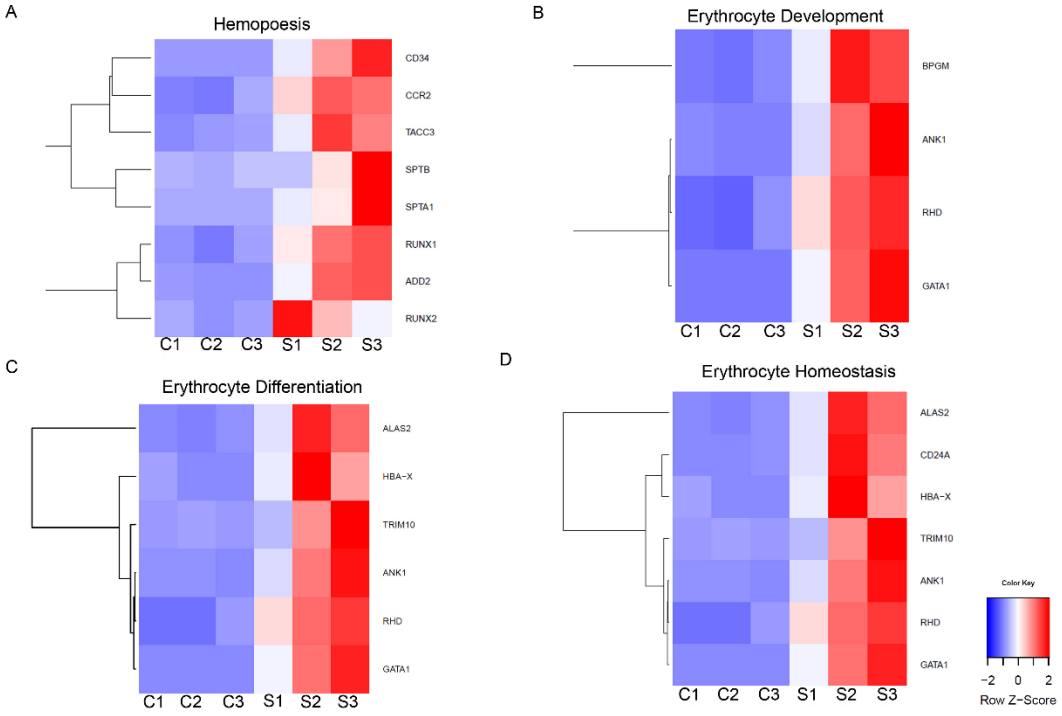

Figure S2: RNA sequence analysis confirms misexpression of genes involved in erythrocyte development in SCD liver. **(A-D)** Pathway analysis revealed increased expression of genes involved in **(A)** Hemopoesis, **(B)** Erythrocyte development, **(C)** Erythrocyte differentiation and **(D)** Erythrocyte homeostasis in the liver of SCD mice compared to control mice liver.

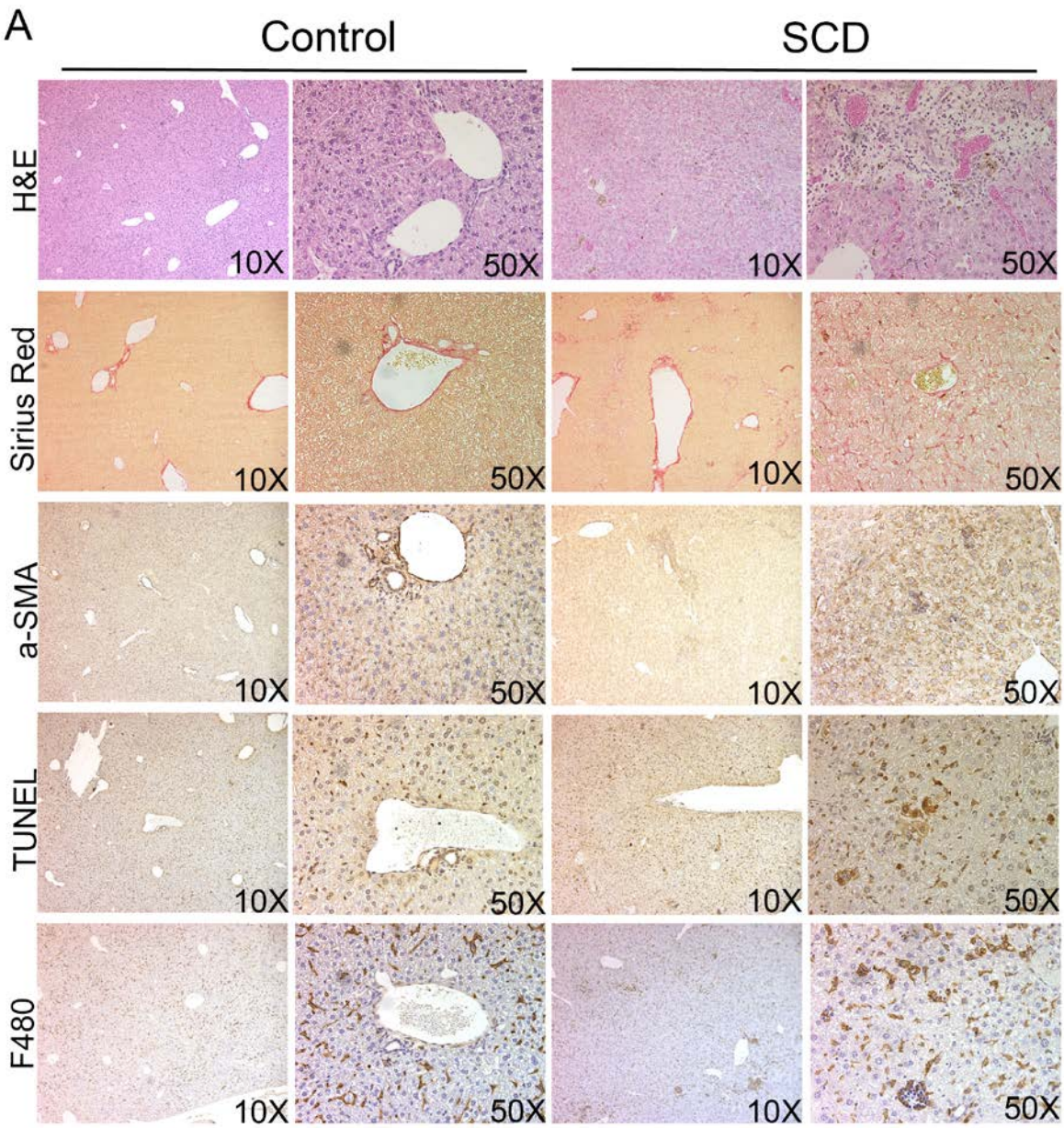

Figure S3: The liver of SCD mice show increased injury, fibrosis, apoptosis and inflammation. **(A)** Immunohistochemical analysis of control and SCD mice liver tissue show increase in dysplastic nodules and dying cells in the liver of SCD mice by H&E staining, Sirius red staining indicates increased fibrosis in the liver of SCD mice. α-SMA staining exhibited hepatic stellate cell activation in the liver of SCD mice. TUNEL staining indicates increased hepatocyte death in

the liver of SCD mice.F4/80 staining exhibit increased inflammation in the SCD mouse tissue as compared to control liver tissue.

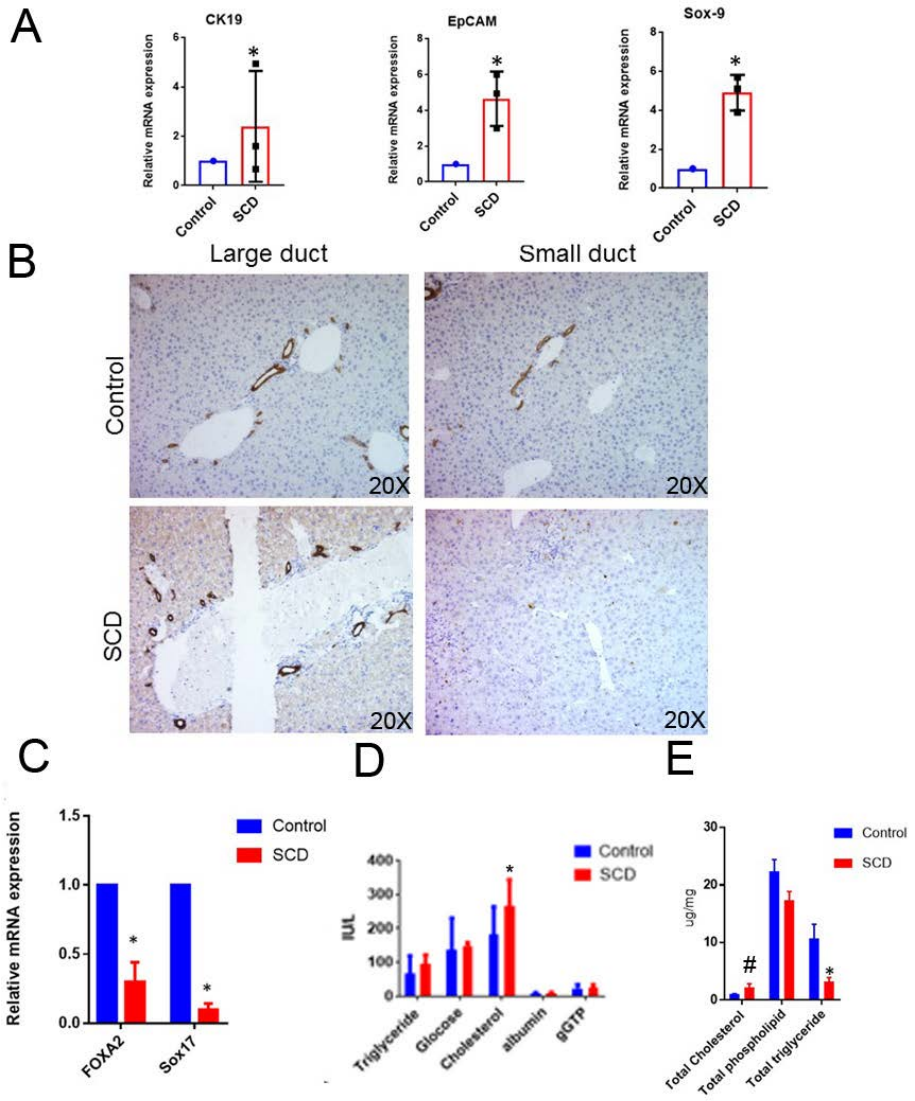

Figure S4: Analysis of ductular reaction in SCD mice liver. *q*RT-PCR analysis reveals significant increase in **(A)** CK-19, EpCAM and Sox-9 mRNA expression in the liver of SCD mice. (B) Immunohistochemical analysis of with CK-19 staining showing large and small ducts in Control liver. Similarly large and small ducts of SCD livers are shown in parallel respectively.

(**C)** qRT-PCR analysis shows significant reduction in mRNA levels of small duct markers FOXA2 and sox17 in the liver of SCD mice. **(D)** Analysis of hepatic cholesterol, phospholipids and triglycerides in control and SCD mice.* denotes P=0.05, # denotes P=0.2.

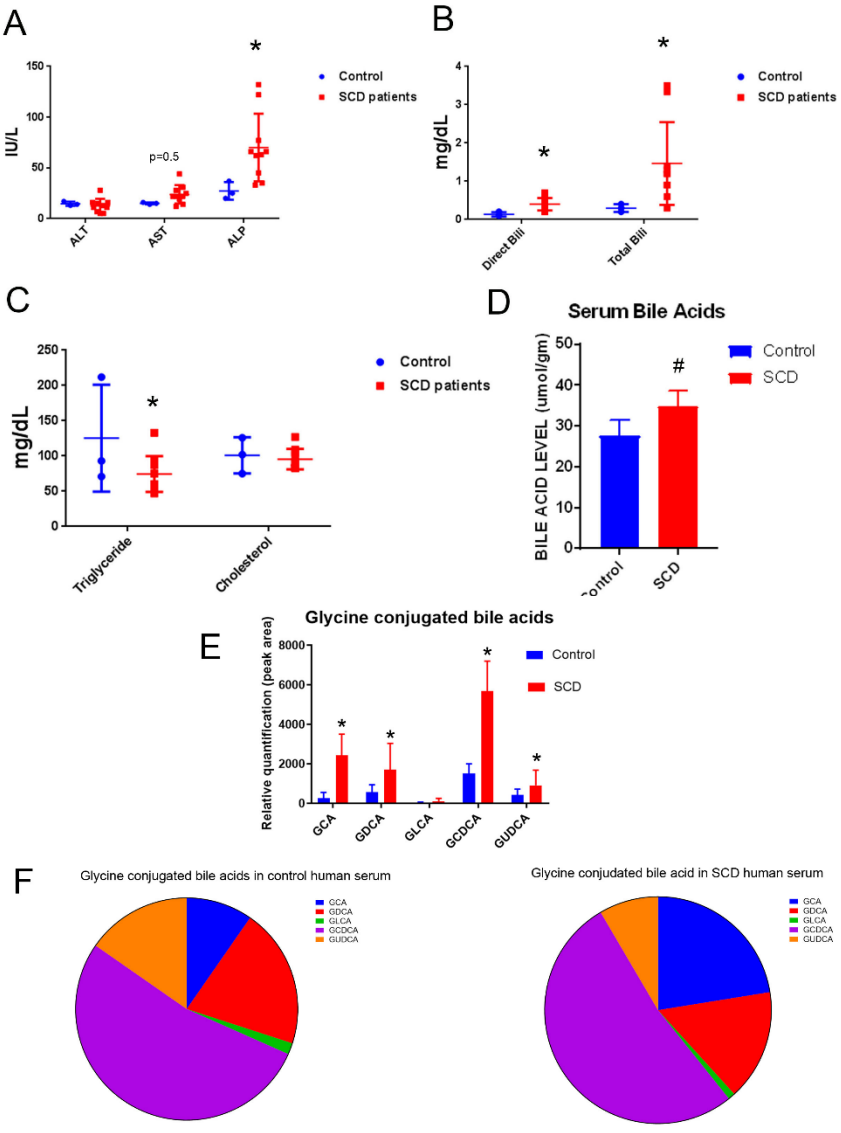

Figure S5: Human validation of SCD mice data. (A) Serum biochemical analysis of liver enzymes ALT, AST and ALP in control and SCD patients (n=10). (B) Serum analysis of direct and total bilirubin levels in control (n=5) and SCD patients (n=10). (C) Analysis of serum triglyceride and cholesterol in control (n=5) and SCD patients (n=10) shows low triglycerides in SCD patients. (D)

SCD patients have increased total serum bile acids (n=10) compared to controls (n=5). (E) Bile acid species analysis of control human serums samples (n=4) and SCD human serum samples (n=4) shows increased GCA, GCDCA and GUDCA in the serum of SCD patients. Pie chart showing bile acid species analysis of control (F) and SCD patient's (G) serum samples. Altered bile acid pool in SCD patients' results in a higher percentage of GCA, GCDCA and GUDCA when expressed qualitatively as a percentage of total BA. * denotes P=0.05. # denotes 0.6.

Supplemental table and legends

Table 1: Clinical characterization of human subjects used in this study

	Control	SCD
Male/Female	3/2	6/4
Hemoglobin (g/dL)	12	9.06
Hematocrit (%)	40.43	25.67
White Blood Cells (k/dl)	5.12	9.87
%Neutrophils	NM	55.2
Neutrophil counts (k/ul)	NM	6.89
Platelets	222.32	328.4
%of HbF	NM	13.96
%HbS	NM	58.23
Genotypes		
SS	0/4	10/10
AS	1/4	0/10
AA	3/4	0/10
SS/β^{α}	0/5	0/10

Table 2: Age of SCD patients used in this study

Demographic Variable				
Total Number of SCD Patients in Each Age Group				
Age	18–24 years	25–44 years	45–64 years	≥65 years
Male	2	1	0	0
Female	2	3	2	0

Supplemental Movie Legends

Movie S1. Visualization of blood flow in a control mouse after administration of TXR- dextran prior to imaging. The sinusoids in control mouse liver visualized by carotid artery injection of TXR- dextran (red). Blood flow appears continuous. Original acquisition rate.

Movie S2. Visualization of blood flow in a control mouse after administration of TXR- dextran prior to imaging. The sinusoids in control mouse liver visualized by carotid artery injection of TXR- dextran (red). Blood flow is continuous. Original acquisition rate.

Movie S3. Visualization of blood flow in a control mouse after administration of TXR- dextran prior to imaging. The sinusoids in control mouse liver visualized by carotid artery injection of TXR- dextran (red). Blood flow appears continuous. Original acquisition rate.

Movie S4. Visualization of blood flow in a SCD mouse after administration of TXR- dextran prior to imaging. The sinusoids in SCD mouse liver visualized by carotid artery injection of TXR-dextran (red). Here the blood flow is occluded at regions which appears dark due to lack of flow. Original acquisition rate.

Movie S5. Visualization of blood flow in a SCD mouse after administration of TXR- dextran prior to imaging. The sinusoids in SCD mouse liver visualized by carotid artery injection of TXR-dextran (red). Here the blood flow is blocked at regions which appears dark due to lack of flow. Original acquisition rate.

Movie S6. Visualization of blood flow in a SCD mouse after administration of TXR- dextran prior to imaging. The sinusoids in SCD mouse liver visualized by carotid artery injection of TXR-dextran (red). Here the blood flow is restricted at regions which appears dark due to lack of flow. Original acquisition rate.

Movie S7. Visualization of blood and bile trafficking in a control mouse after administration of Texas red dextran and CF 1 minutes prior to imaging. The sinusoids in control mouse liver visualized by carotid artery injection of Texas red dextran (red). Hepatocytes and biliary canaliculi are enriched in CF (green). Texas Red Dextran and CF localization appeared to be mutually exclusive at this time point. Original acquisition rate.

Movie S8. Time series video exhibiting the flow of Texas red dextran and CF through liver sinusoids and bile canaliculi at 3 min post administration in a control mouse.Control mouse liver imaging 4 minutes after carotid artery injection of CFDA. The sinusoids are visualized by IV injection of Texas red dextran (red). The biliary canaliculi are nicely outlined with CF (green). No CF staining is seen in hepatocytes. Texas Red Dextran and CF localization is mutually exclusive at this time. Original acquisition rate.

Movie S9. ***Visualization of blood and bile flow in a control liver through liver sinusoids and bile canaliculi using texas red dextran and CF respectively at 10 minutes post administration.***
Normal liver sinusoids in a dWT mouse visualized by carotid artery injection of Texas red dextran (red). The bile ducts are visualized with CF (green). The biliary canaliculi are nicely outlined with

CF (green). No CF staining is seen in hepatocytes. Texas Red Dextran and CF localization is mutually exclusive at this time. Original acquisition rate.

Movie S10. Visualization of blood and bile trafficking in a SCD mouse after IV administration of Texas red dextran and CF 1 minutes prior to imaging. The sinusoids in SCD mouse liver visualized by carotid artery injection of Texas red dextran (red). Hepatocytes and biliary canaliculi are enriched in CF (green). Texas Red Dextran and CF localization appeared to be mutually exclusive at this time point. Original acquisition rate.

Movie S11. Time series video exhibiting the flow of Texas red dextran and CF through liver sinusoids and bile canaliculi at 3 min post administration in a SCD mouse.SCD mouse liver imaging 3 minutes after carotid artery injection of CFDA. The sinusoids are visualized by carotid artery injection of Texas red dextran (red). The biliary canaliculi are nicely outlined with CF (green). CF staining continues to enrich in the hepatocytes also at this time point. Texas Red Dextran and CF localization is mutually exclusive at this time. Original acquisition rate.

Movie S12. ***Visualization of blood and bile flow in a SCD liver through liver sinusoids and bile canaliculi using texas red dextran and CF respectively at 10 minutes post administration.***
Liver sinusoids in a SCD mouse visualized by carotid artery injection of Texas red dextran (red). The bile ducts are visualized with CF (green). CF fluorescence is still lighting up the hepatocytes along with bile canaliculi suggestive of delayed bile transport. Original acquisition rate.

Movie S13. ***Visualization of blood and bile flow in a SCD liver through liver sinusoids and bile canaliculi using texas red dextran and CF respectively at 5 minutes post administration.***

Liver sinusoids in a SCD mouse after 12 weeks of visualized by carotid artery injection of Texas red dextran (red). The bile ducts are visualized with CF (green). No sinusoidal vasoocclusion was seen in the FOV examined. Original acquisition rate.

Movie S14. ***Visualization of blood and bile flow in a SCD liver through liver sinusoids and bile canaliculi using texas red dextran and CF respectively at 10 minutes post administration.***

Liver sinusoids in a SCD mouse after 12 weeks of visualized by carotid artery injection of Texas red dextran (red). The bile ducts are visualized with CF (green). No sinusoidal vasoocclusion was seen in the FOV examined. Original acquisition rate.